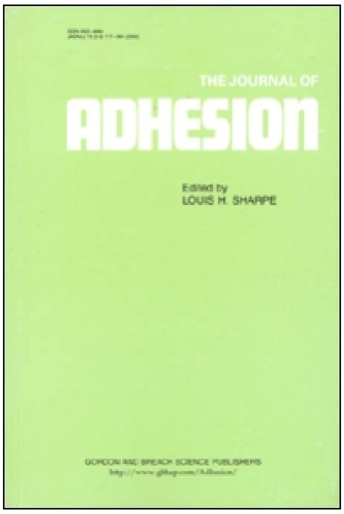

The Journal of Adhesion
Publication details, including instructions for authors and subscription information:
http://www.informaworld.com/smpp/title~content=t713453635

Theoretical Modeling of the Nucleation and Growth of Aluminium Films Thermally Evaporated onto Poly(ethylene terephthalate) Substrate

Y. Travaly[a]; P. Bertrand[a]; G. -M. Rignanese[a]; X. Gonze[a]
[a] Unité PCPM, Université Catholique de Louvain, Louvain-La-Neuve, Belgium

To cite this Article Travaly, Y. , Bertrand, P. , Rignanese, G. -M. and Gonze, X.(1998) 'Theoretical Modeling of the Nucleation and Growth of Aluminium Films Thermally Evaporated onto Poly(ethylene terephthalate) Substrate', The Journal of Adhesion, 66: 1, 339 — 355

To link to this Article: DOI: 10.1080/00218469808009973

URL: http://dx.doi.org/10.1080/00218469808009973

J. Adhesion, 1998, Vol. 66, pp. 339-355
Reprints available directly from the publisher
Photocopying permitted by license only

Amsterdam B.V. Published under license
under the Gordon and Breach Science
Publishers imprint.
Printed in India.

Theoretical Modeling of the Nucleation and Growth of Aluminium Films Thermally Evaporated onto Poly(ethylene terephthalate) Substrate*

Y. TRAVALY**, P. BERTRAND, G.-M. RIGNANESE
and X. GONZE

*Unité PCPM, Université Catholique de Louvain, 1, Pl. Croix-du-Sud,
B-1348 Louvain-La-Neuve, Belgium*

(Received 10 February 1997; In final form 5 September 1997)

The interface between aluminium and poly(ethylene terephthalate) (PET) has been studied using the density functional theory (DFT) formalism within the local density approximation (LDA). An examination of the charge transfers during Al bonding with the polymer functional groups provides a better understanding of the nucleation of the metallic film. Indeed, when reacting with the doubly-bonded oxygen atom of the ester function, the metal particle induces strong modifications in the highest occupied molecular orbitals (HOMOs) as well as in the lowest unoccupied molecular orbitals (LUMOs) of the PET. The shape of the HOMO, HOMO-3 and HOMO-4 of the Al/PET complex confirms the evolution of the phenyl structure to a quinoid structure. We emphasise the extent to which the reactivity of the PET can be modified after Al interaction with the ester function. After losing their aromaticity, the phenyl rings of the polymer are no longer available for subsequent interactions. Hence, we propose that the Al film will then grow following a compact cubic stacking on top of Al atoms already fixed on the ester functions.

Keywords: Metal; polymer; adhesion; chemical bonding; density functional theory; static secondary ion mass spectrometry

---

*Presented at EURADH'96/ADHESION'96 (European Adhesion Conference), Churchill College, Cambridge, UK, 3-6 September, 1996.

**Corresponding author.

INTRODUCTION

Poly(ethylene terephthalate) (PET) is a well-suited material for packaging applications. Its good barrier properties and chemical resistance provide the necessary protection for the packed food. Unfortunately, the as-received polymer properties are typically insufficient for practical applications. One possibility to improve the gas barrier properties consists in depositing an aluminium film several nanometers thick on the polymer film. Therefore, an important quality parameter control for the final product is the adhesion between the metallic film and the polymeric material.

The adsorption process is believed to be the more relevant mechanism of metal/polymer adhesion. We may distinguish physisorption, where no electron transfer between the contacting bodies occurs, from chemisorption in which a chemical interaction (with electron transfer) takes place between the metal and the polymer [1].

Many workers have studied the adhesion of metals to polyesters. XPS results [2, 3] support a mechanism of electron transfer from the Al atoms to the ester functions which act as preferential adsorption sites. Decrease in the shake-up intensity also suggests a loss of aromaticity upon metal deposition. A combination of ISS, RBS, TEM and peel test measurements [4, 5] has shown that the polymer crystallinity may affect the adhesion level: the peel strength mean value is greater for high-crystallinity PET in comparison with low-crystallinity PET. Further, the metallization conditions (rate, pressure) are also important regarding the quality of the interface. Indeed, for decreasing metallization pressure and increasing deposition rate, the Al mean grain size increases. HREELS [6] results confirmed XPS findings but also suggest an Al bonding with two oxygen atoms. Using static SIMS [7, 8], we reported an uniform coverage of the PET substrate and, hence, an initial layer-by-layer growth of the metallic film. The results evidenced an interaction with the doubly-bonded O of the ester functions until saturation, after which the growth kinetics slows down. We also noticed a drastic decrease in the secondary SIMS intensity related to the aromaticity during the first metallization steps.

In this work, we used a theoretical approach to analyze the charge transfer mechanisms and modifications in the PET orbitals upon Al deposition. For that purpose, we performed calculations in the framework of the density-functional theory (DFT) [9], within the local density approximation (LDA) [10]. As a model for the polymer, we used PET in the *trans*-conformation consisting of one monomer in a box subjected to periodic boundary conditions such that a 1D-isolated chain is formed. After calculations on the isolated chain, several Al atoms are introduced in the surroundings of the candidate interaction sites in order to model the nucleation process. Then we tried to simulate the growth of an Al metallic film starting from metal atoms already fixed on the PET. We present results in which interactions with the oxygen and phenyl functionalities have been evaluated. We also evaluated the changes in the charge density distribution upon metallization together with a partial relaxation of the Al distance to the polymer.

THEORETICAL DETAILS

Geometry

The segment of the polymer chains used to build up the unit cells related to the PET chain conformation is depicted in Figure 1. The structure presents a planar conformation (except for the hydrogen atoms, all atoms are in a plane) with a *trans*-conformation of oxygen atoms in the glycol segment. The bond angles and bond lengths used to initiate our calculations originate from the geometry optimized on dimethylterephthalate, using the Austin Model (AM1) semiempirical Hartree-Fock method [11]. Some of these parameters are given in Table I. We also neglected interactions between neighboring chains with respect to the direction lying along the surface plane and perpendicular to the polymer backbone (see Fig. 1). Therefore, we have created a vacuum region about 16 Å wide, between periodic cells, wide enough so that adjacent chains do not interact.

Even though it is now well established that Al atoms react with the doubly-bonded oxygen of the PET unit, two or four metal atoms were first added to the system to test their interaction with the PET. Since geometry optimization was not performed when these atoms were added, our theoretical results, regarding the Al adsorption energies, need further refinement. By contrast, the analysis of the charge density

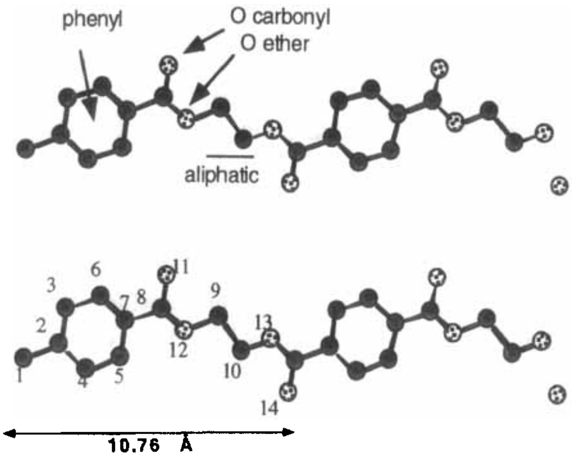

FIGURE 1 Molecular and geometric structure of the repeating monomer of PET. The H atoms are not shown.

TABLE I Bond lengths (in Å) and bond angles (in degrees) for the PET molecule. The atom labeling in this table refers to that shown in Figure 1

Geometrical parameters			
bonds lengths [*Å*]		*bonds angle* [*degrees*]	
C2—C3	1.4016	C4—C2—C3	120.016
C3—C6	1.4020	C2—C3—C6	119.997
C6—C7	1.4021	C3—C6—C7	119.940
C7—C5	1.4017	C6—C7—C5	120.041
C5—C4	1.4007	C7—C5—C4	119.992
C4—C2	1.2349	C5—C4—C2	120.014
C8—O11	1.4018		
C8—O12	1.2344	C8—O12—C9	119.997
O12—C9	1.4351	C10—O13—C1	120.008
C10—O13	1.2341		
O13—C1	1.2344		
C1—O14	1.2349		

and orbitals weakly depend on the fine tuning of the geometry. Nevertheless, it is to be noted that we have elected to consider a set of about 10 different Al/PET configurations and the trends of our results in terms of adsorption energies reproduce quite well those of Calderone *et al.* [12]. Some of the Al_n/PET complexes, on which calculations have been performed, are shown in Figure 2.

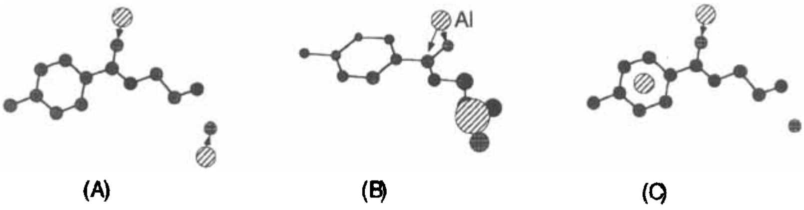

FIGURE 2 Side views of the most favorable binding configurations involving Al atoms and PET functional groups. The specific interactions that may be considered in each case are depicted in the figure by arrows.

Methodology

The density functional theory as implemented in the Corning Code [13] was used for the calculations performed in this study. The exchange-correlation energy within the local density approximation (LDA) was generated from the Ceperely and Adler electron gas data [14] parameterized by Teter [13]. Separable, extended norm-conserving, *ab initio* pseudo potentials represented the ionic cores [13]. The wave functions were expanded in a large set of plane waves and special *k* points were used to sample the Brillouin zone (BZ). Therefore, the BZ sampling and the number of plane waves were carefully checked. We used typically 2*k* points in the irreducible part of the Brillouin zone (4*k* in the full BZ) for total energy calculations and an energy cut-off of 18 Ha (about 70,000 plane waves). Convergence errors are expected to be lower than 0.01 eV.

The formation of the metal/polymer interface is expected to result from a strong intermixing of the metal and the polymer orbitals. Hence, a detailed comprehension of both the metal, polymer and metal/polymer band structures is required for a full understanding of the Al/PET interaction. In this study, allocation of the valence electrons in the Al/PET systems was achieved on the basis of the Kohn-Sham equations [15]. In such a procedure, on the basis of the wave functions used to construct a particular band or a group of bands, we calculated the corresponding valence electronic density. The nature of the molecular orbitals from which the valence electrons originate is then deduced from the shape and the location inside the cell of the corresponding partial density. In the remainder of this paper, this procedure is referenced as "Band-by-Band" analysis.

The relative stability of different binding configurations was evaluated from the adsorption energy per metal atom interacting with the PET functions under consideration. This energy is calculated from the difference between the Al_n/PET total energy and the separate polymer and metal total energies divided by the number of interacting metal atoms (n).

RESULTS

PET Electronic Properties

The complete band structure calculated for the computed density of valence state (DOVS) for PET present 36 doubly-occupied valence bands. As a matter of fact, the PET monomer unit contains 10 carbons (*i.e.* 40 valence electrons), 4 oxygens (*i.e.* 24 valence electrons) and 8 hydrogens (*i.e.* 8 valence electrons). Therefore, 36 doubly-occupied bands are necessary to contain the polymer valence electrons. It has been observed that these bands are essentially flat indicating that the electronic states in PET are highly localized within each unit cell. A detailed understanding of the allocation of the C, O and H valence electrons on the polymer valence bands is achieved using the band-by-band analysis procedure described in methodology section. The most important features in the valence band of PET identified by this procedure were published elsewhere [16]. Examination of the highest-occupied and lowest-unoccupied orbitals as well as others in the same energy region, revealed the following: (1) the highest-occupied molecular orbital (top of the valence band region) minus three bands (HOMO-3, ΔE(HOMO; HOMO-3) = −0.794 eV), that is the band number 33, and the HOMO-2 (band 34, ΔE (HOMO; HOMO-2) = −0.624 eV) originate from the π electronic level delocalised over the benzene and from the p electronic level of the doubly-bonded O atom (*O-d*); (2) the HOMO-1 (band 35, ΔE(HOMO; HOMO-1) = −0.265 eV) and HOMO (band 36) arise from the *O-d* 2p atomic contributions; (3) the first excited state of the polymer or lowest-unoccupied molecular orbital (LUMO) is mostly built from the π orbitals delocalised over the carbons connecting the phenyl and ester groups. There is also a contribution from the *O-d* 2p orbitals that are perpendicular to the polymer backbone; (4) the LUMO + 1 (+ 1.171 eV from the LUMO level) originates from the contribution of the π orbitals delocalised over the C3—C6 and C4—C5 linkages; (5) finally, LUMO + 2 (+ 1.93 eV from the LUMO level) has a strong contribution from the O 2*p* orbitals. Other significant features of the polymer valence band spectrum are summarized in Table II.

Note that the band energies clearly show that the five highest occupied orbitals are very close in energy. Hence, it is mandatory to consider also orbitals other than the frontier orbitals.

Al/PET Electronic Properties

Binding Configurations

As mentioned above, different binding configurations were considered in order to investigate the chemical interactions occurring at the Al/PET interface and, hence, the nucleation of the metallic film. For that purpose, we have selected several starting configurations which encompass interactions with the different sites of interaction (oxygen, aliphatic, phenyl) available on the PET surface. Some of the selected structures are presented in Figure 2. In all cases, the C=O groups are

TABLE II Main contributions to the most important features in the valence band of a semi-crystalline PET film. Labels correspond to those used in Figure 1

Band number	*Main atomic contributions*
1-4	Ether O 2*s* bonding and anti-bonding (1-2) Carbonyl O 2*s* bonding and anti-bonding (3-4)
5-9	C 2*s* totally bonding Ether O 2*p* C—O from C8—O12—C9 and C10—O13 linkages σ orbitals with one nodal plane
10-18	σ orbitals with two nodal planes Ether O 2*p* C—C bonds connecting aromatic and ester groups
19-25	σ orbitals with three nodal planes πC=O C—H and C—C bonds from the aromatic ring
26-32	O 2*p* C—C and C—H
33-36	π delocalised orbitals of benzene (33-34) carbonyl O 2*p* (35-36)

implicated. In system A and B, each doubly-bonded oxygen atom is attacked by an Al atom to form an Al–O–C complex with the metal-oxygen-carbon angle being fixed at 180° and 90°, respectively. We point out that in complex B, Al–C interactions have to be taken into account. In system C, one Al atom interacts with the C═O group, the other one with the benzene ring. The stability of these structures was evaluated from the corresponding adsorption energy per metal atoms as previously discussed in the theoretical details section. The Al–O distance was arbitrarily fixed at 1.5 Å in order to draw the reactivity scale of the PET functional groups towards the incoming metal atoms.

The results show that complexes B (–0.26 eV) and C (–0.91 eV) are less stable than system A (–1.21 eV) by –0.96 and –0.3 eV per Al atom, respectively. Hence, although a direct interaction with the ring is favorable, the results suggest that this type of interaction is partly responsible for the lower stability of the resulting complex in comparison with complex A.

Orbitals Mixing

Chemisorption is believed to be the more relevant mechanisms for the formation of the metal/polymer interface. The process implies a strong intermixing of the metal and the polymer orbitals, concomitant with a flow of electronic charge from the occupied levels of the metal to the unoccupied levels of the PET. Hence, analysing the HOMOs of the PET and Al/PET complexes as well as the LUMOs of the PET, we aim to understand fully the mechanism by which the metal reacts with the polymer functionalities. The composition of these molecular orbitals in both isolated PET and Al_2/PET complex suggests strong modifications in the molecular orbitals upon Al bonding with the C═O groups (Fig. 3(a)). As a matter of fact, due to the charge coming from the HOMO of the metal populating the π^* level of the PET (LUMO, LUMO+1 and LUMO+2), mixing of the PET molecular orbitals occurs. The molecular orbitals originating from the carbonyl O $2p$ molecular orbitals as well as from the π electronic levels of the benzene ring do not contribute any more to the Al_2/PET band structure. HOMO, HOMO-3 and HOMO-4 of the Al_2/PET complex suggest some change in the aromatic character of the PET. In fact, the shape

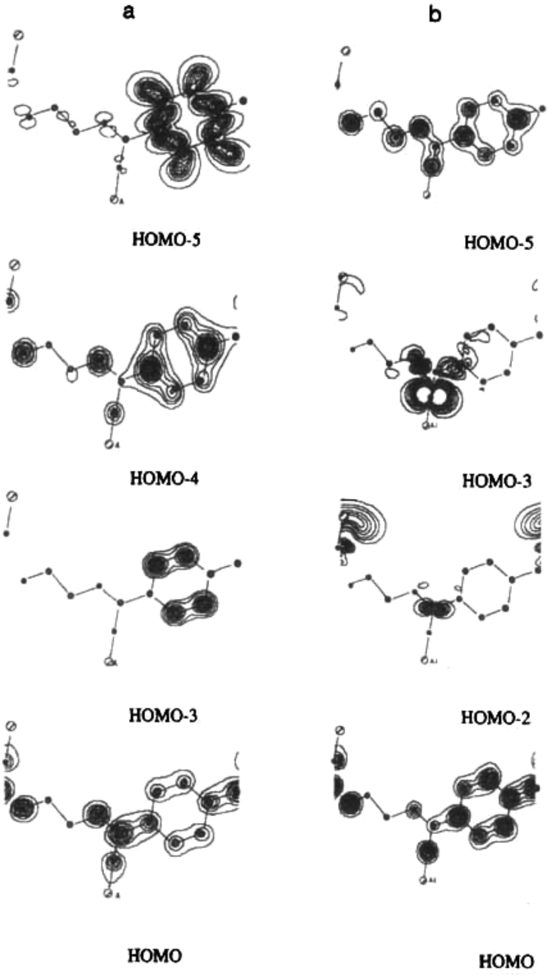

FIGURE 3 Chemical structure of the Al_2/PET complex and the LDA molecular orbitals of the uppermost occupied orbitals of the complexes A (a) and C (b).

of these orbitals indicates a possible evolution of the phenyl structure to a quinoid structure. These observations match those of Calderone *et al.* [12] based on changes in the geometrical parameters upon Al bonding. We emphasized the extent to which the reactivity of the PET is modified after Al interaction with the C=O groups. Indeed, due to the change in the aromatic character of the PET, the phenyl rings are no longer available for subsequent interactions. Concerning Al interaction with both C=O and phenyl groups (system C) (Fig. 3(b)), we also observed strong modifications in the frontier orbital composition. The HOMO-3 of the Al_2/PET complex originates from the carbonyl O 2*p* orbital related to the carbonyl group undisturbed by the incoming Al atom. This orbital also contributes to the HOMO-2 of the metallized polymer concurrently with the atomic contribution from the Al–O–C complex involving the interacting C=O group. Finally, some modifications are qualitatively the same as those already observed in complex A: HOMO and HOMO-5 involved in system C are similar to the HOMO and HOMO-4 of system A; the π electronic levels delocalised over the benzene ring are also depopulated. However, our results do not evidence an evolution of the phenyl ring to the aforementioned quinoid structure. Also, these results do not clearly display a diene structure as proposed by Calderone *et al.* [12] to model a direct interaction with the phenyl ring.

Relaxation of the Al to PET Distance

It seems to be reasonable to believe that the Al distance to the polymer may affect the amplitude of the adsorption energy of the metal atom on the specific interactions sites of the PET. In order to evaluate the extent to which the interatomic distance between the contacting bodies influences the interaction energy, the adsorption energy of complex A (the most favorable case) was calculated for a set of interatomic distances ranging from 1.2 Å to 2.2 Å. The equilibrium distance was obtained as the minimum of the adsorption energy curve *versus* interatomic distance. The energetic result for system A is presented in Figure 4. The adsorption energy per metal atom for an optimal distance of 1.65 Å is found to be −2.12 eV; that is to say, an adsorption energy difference of −0.91eV for an Al–O distance varying from 1.5 Å (distance used in the starting complexes) to 1.65 Å. Even if this result underlines the necessity of an optimization of the geometrical parameters for providing more accurate adsorption energy values, we will show in the next section that the Al–O distance weakly influences the amplitude of the charge transfers.

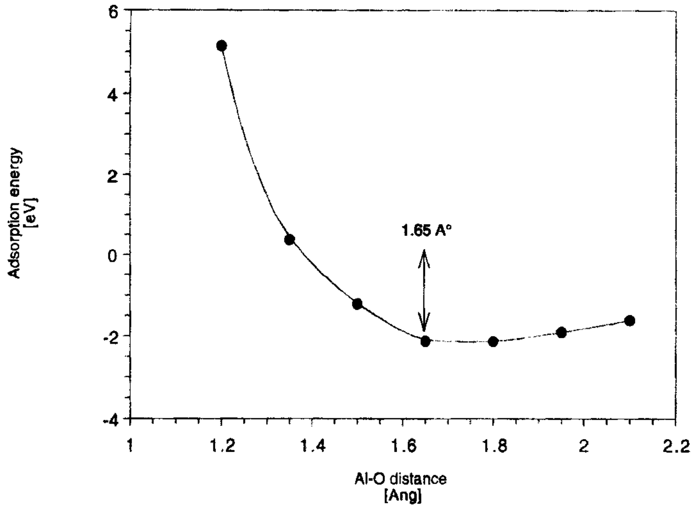

FIGURE 4 Evolution of the Al adsorption energy against the metal-to-PET distance. The calculations were performed for system A.

Charge Transfer

In order to account, firstly in a qualitative manner, for the modifications in the charge distribution, we have calculated the polymer, the metal and the metal/polymer densities of charge on the basis of the wave functions generated by the Corning Code. Then the isolated polymer and metal densities were subtracted from the metal/polymer density. The results are presented in Figure 5 for complexes A and C. The effects specific to the charge transfer are labeled by " + " for increased a density regions and "–" for depleted density regions.

In the binding configuration related to complex A, it is seen that the charge transferred upon Al bonding resides in the vicinity of the carbon bonds connecting the aromatic ring to the ester group as well as over the C3—C6 and C4—C5 bonds inside the ring. We also notice an increase in the electronic density in the neighborhood of Al–O linkages. Finally, in some regions, we observed a net depletion in the valence electronic density.

In order to quantify the changes in the charge distribution inside the PET unit cell upon complexation with Al, we have divided the space

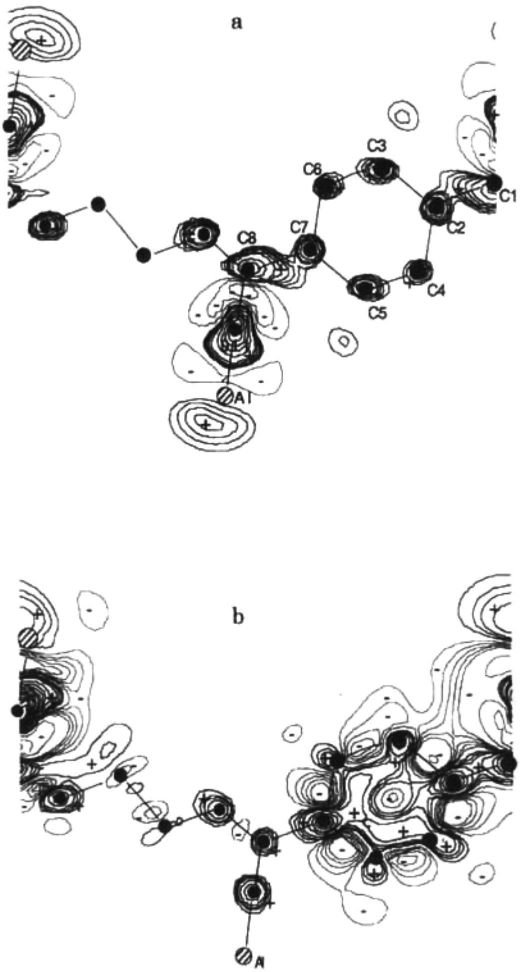

FIGURE 5 Contour plot of the charge transfer due to the interaction between Al atoms and (1) the PET C═O groups; (2) both C═O and phenyl functions. "+" label indicates increase in the density and, "−" indicates depletion in the density. Atomic locations are also shown in the figure.

according to the decrease or increase of charge density due to bonding. In particular, we have isolated four pockets labelled R1, R2, R3 and R4 in which the charges increases.

For an Al−O distance of about 1.5 Å (near the minimum adsorption energy value), after bonding with Al, the density over the carbon bonds connecting the phenyl ring to the ester functions (regions R1 (C1—C2) and R2 (C7—C8)) increases by +0.25 |e| and +0.18 |e|, respectively. Also the density over the C3—C6 and C4—C5 (R3, R4) of the phenyl ring increases by +0.03 |e| and +0.03 |e|. Hence, the modifications in the charge distribution induce a net increase of +0.49 |e| on the phenyl ring (summation over R1, R2, R3, and R4). This charge resides almost completely over the bonds connecting the ring to the ester functions.

Varying the distance from 1.5 Å to 1.65 Å, the density over the ring remains the same with weak modifications in the charge distribution over the above regions. Indeed, in the vicinity of the bonds connecting the benzene and ester functions, the density is reduced from +0.43 |e| to +0.4 |e| while in the vicinity of C3—C6 and C4—C5 bonds, the density increases from +0.06 |e| to +0.08 |e|. It is to be noted that the Al–O distance does not influence drastically the charge distribution as compared with its influence on the adsorption energy. In other words, a complete charge transfer is achieved as soon as the Al distance to the PET function under study is short enough to permit bond establishment.

Growth of the Al Film

Based on the above results, we assumed that the first incoming Al atoms interact with the C═O groups. For subsequent incident particles, we supposed a compact cubic stacking (FCC) on top of Al atoms already fixed on the C═O groups. We have elected to consider a cubic *F* stacking in which the compact planes are perpendicular to the ternary axis of a cube. In this case, the growing of the metallic film begins with a cluster of three Al atoms lying flat on the PET substrate. We emphasise that another possibility could be a cubic *F* stacking with the compact planes perpendicular to the quaternary axis. This stacking supposes a cluster of four Al atoms lying flat on the substrate. It would be interesting to evaluate the energetics of this second possibility in order to make a comparative study between these two stackings. For the structure shown in Figure 6, we set the Al–Al distance to 2.36 Å, which is the value taken from bulk data. Energetic results show that for one Al-cluster growing on top of an Al atom already fixed on a C═O group (the first Al atom is collinear to the C═O group, see

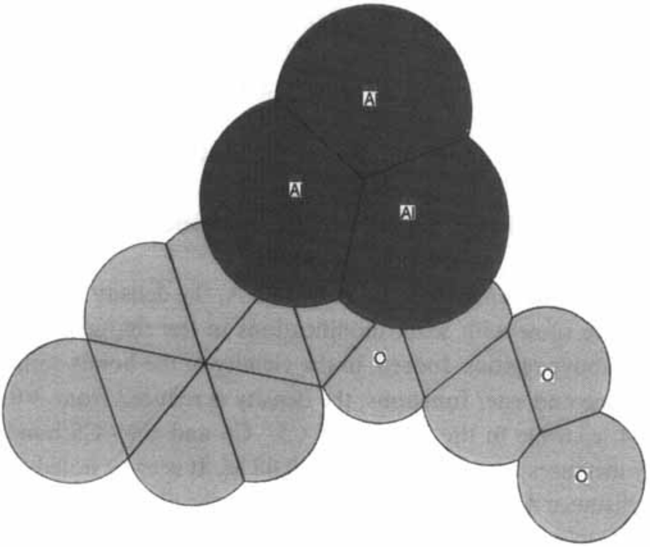

FIGURE 6 Growth of the metallic film. We assumed an initial compact cubic *F* stacking, with the compact planes perpendicular to the ternary axis of a cube.

case A), the corresponding adsorption energy is −0.25 eV per Al atom. With two Al-clusters growing, respectively, on top of an Al atom fixed on each C=O group, the adsorption energy is also −0.25 eV per Al atom.

DISCUSSION

We now discuss these theoretical results in view of experimental results obtained by two of us and presented in Refs. [8] and [9].

These static SIMS (SSIMS) results recorded on PET metallized samples indicated strong modifications in the SSIMS intensity related to the PET oxygenated fragments. The data also pointed to a loss of aromaticity induced by the metal deposition during the first metallization steps. Finally, we noticed that the SSIMS spectra, recorded for the PET, are also consistent with a two-step growth kinetics of the metal layer. As a matter of fact, the first Al atoms, until a 4.5×10^{14} Al atoms·cm^{-2} coverage, are expected to interact strongly with the C=O groups. During this stage, the charge transferred from the HOMO of the metal to the LUMOs of the PET induces a partial loss of aromaticity without disrupting the ring. *Ab initio* findings show that this change in the aromatic character of the polymer originates from the π levels of the PET that become depopulated while the π^* unoccupied delocalised orbitals are being populated. This kind of interaction, accompanied by an increased localization of the electronic charge over the ring, results in the formation of a rather stable "Al−O−C" structure. As a result of the charge transfers, modifications in the fragmentation mechanism of the PET repeat unit occur. These modifications are due to both reinforcement and weakening of some typical bonds and may account for the observed decrepancy in the SSIMS intensity related to the 76 Da fragments during the first metallization steps. Based on quantum-chemical calculations, Calderone *et al.* [12] have shown that the phenyl ring can lose its aromatic character upon Al bonding with the two C=O groups. In this case, they reported the formation of quinoid structures. In such a complex, the bond lengths which connect the ester groups to the phenyl ring shorten from 1.505 Å to 1.384 Å. This result indicates that the single bonds now present a double bond character. Our results corroborated quite well the formation of such products. We also noticed that the TOF-SIMS analyses performed in the high mass resolution mode (HRM) on metallized and unmetallized PET samples confirmed the central role of oxygen-containing fragments. Also, the TOF-SIMS results evidenced the emission of "C_2OAlH_2" fragments instead of "Al−O−C" fragments. In order to explain this result, one can consider the modifications in the PET fragmentation scheme upon Al deposition. As a matter of fact, when reacting with the C=O groups, the charge transferred from the metal to the polymer induces: the weakening of certain bonds: C7—C6 and C7—C5; the reinforcement of other bonds: C7—C8 and, finally, the establishment of an Al−O bond. Hence, the fragment observed with the TOF-SIMS apparatus could be a C(7)—C(8)—O(11)—Al—H_2 fragment (see Fig. 6).

At higher coverage, beyond a 4.5×10^{14} Al atoms·cm^{-2} coverage, that is to say when all the available C=O groups have been attacked, interactions with the phenyl rings could appear but the modifications due to the C=O group attack may prevent this kind of interaction.

In fact, it has been noticed that an interaction with the C=O group induces the destruction of the potential interaction sites constituted by the phenyl rings. Therefore, we do not exclude the possibility of a direct interaction of Al atoms with the phenyl rings with the limitation that it occurs in the first metallization steps. We believe that during the advanced metallization steps the metal atoms react with those which are already attached to the polymer's doubly-bonded O of the ester groups. Hence, the change in the growth kinetics after saturation of the available ester sites results from the multiplication of Al–Al interactions.

CONCLUSION

In order to understand the microscopic behavior of the Al/PET interface, we performed a theoretical (density functional theory, plane wave basis set and pseudopotentials) study of the Al/PET interface formation. Thanks to a band-by-band analysis of the PET and Al/PET molecular orbitals, we provided information on the manner in which changes in the aromatic character of the polymer occur. The metal atoms are also found to bind to the phenyl rings but the resulting compounds are less stable than those formed upon Al bonding with the C=O groups. Further, we believe that such an interaction takes place only if it occurs simultaneously with interactions with the C=O groups. Our results also highlight the importance of the metal-to-polymer distance on the metal adsorption energies. On the contrary, the above parameter weakly affects the amplitude of the charge transfers.

The theoretical results correlate quite well with experimental findings. Indeed, these results confirmed the SSIMS observations: the metal atoms tend to bind preferentially to the carbonyl sites of the PET. Such an interaction modified drastically the PET fragmentation scheme during the SIMS analyses and as a result, loss of aromatic ions occurs. The theoretical results indicated changes in the aromatic character of the polymer upon Al bonding. Further, after saturation of the PET carbonyl oxygen has been reached, it is reasonable to consider that the growth of the metallic film starts from the Al atoms already attached on the C=O functions.

Acknowledgment

This work is supported by the Belgian program on Interuniversity Poles of Attraction initiated by the Belgium State (PAI-IUAP 49 and P4/10).

References

[1] Lee, L. H., *J. Adhes. Sci. Technol.* **5**(1), 71, (1991); Lee, L. H., *J. Adhesion* **37**, 187, (1992); Lee, L. H., *J. Adhesion* **46**, 15 (1994).

[2] Bou, M., Martin, J. M., LeMogne, Th. and Vovelle, L., *Appl. Surf. Sci.* **47**, 149.

[3] Droulas, J. L., Jugnet, Y. and Tran, Minh Duc, *Metallized Plastics* **3**, 123.

[4] De Puydt, Y., Bertrand, P. and Lutgen, L., *Surf. and Interf. Anal.* **12**, 486 (1988).

[5] De Puydt, Y., Phuati, P. and Bertrand, P., in proceedings of *Workshop on Interfaces in New Materials*, Grange, P. and Delmon, B. (Elsevier Appl. Sci., London 1991) p. 149.

[6] Novis, Y., Degosserie, N., Chtaïb, M., Pireaux, J. J., Caudano, R., Lutgen, P. and Feyder, G., *J. Adhes. Sci. Technol.* **7**, 699 (1993).

[7] Bertrand, P., Travaly, Y. and de Puydt, Y., *Metallized Plastics* 4, *Fundamentals and Applied Aspects* Mittal, K. L. Ed., M. Dekker Publ., Chap 14, 141 (1997).

[8] Travaly, Y. and Bertrand, P., *Surf. and Interf. Anal.* **23**, 328 (1995).

[9] Hohenberg, P. and Kohn, W., *Phys. Rev. B*, **864**, 136 (1995).

[10] Kohn, W. and Sham, L., *Phys. Rev. A*, **1133**, 140 (1965).

[11] Dewar, M. J., Zoebish, E. G., Healy, E. F. and Stewart, J. J. P., *J. Am. Chem. Soc.* **107**, 3902 (1985).

[12] Calderone, A., Lazzaroni, R. and Brédas, J. L., *J. Chem. Phys.* **102**, 4299 (1995).

[13] Allan, D. C. and Teter, M. P., Corning Inc.

[14] Ceperley, D. M. and Alder, B. J., *Phys. Rev. Lett.* **45**, 566 (1980).

[15] Payne, M. C., Teter, M. P. and Allan, D. C., Arias, T. A. and Joannopoulos, J. D., *Rev. Mod. Phys.* **64**(4), 1046 (1992).

[16] Travaly, Y., Bertrand, P., Gonze, X. and Rignanese, G.-M., *Proc. ICPSI-2: from model to real systems* Namur, Aug. 12–16 (1996).